

# ON THE PERFORMANCE OF TIKHONOV, TOTAL VARIATION AND BALANCED TIKHONOV-TOTAL VARIATION REGULARIZATIONS IN NONLINEAR SEISMIC CROSS-HOLE TOMOGRAPHY

YASE SOUFI<sup>1</sup>, MOHAMMAD ALI RIAHI<sup>2</sup> and REZA HEIDARI<sup>1</sup>

<sup>1</sup> *Islamic Azad University, Science and Research Branch, Tehran, Iran.*

<sup>2</sup> *Institute of Geophysics, University of Tehran, Tehran, Iran. mariahi@ut.ac.ir*

(Received August 4, 2023; accepted September 28, 2023)

## ABSTRACT

Soufi, Y., Riahi, M.A. and Heidari, R., 2023. On the performance of Tikhonov, total variation and balanced Tikhonov-Total Variation regularizations in nonlinear seismic cross-hole tomography. *Journal of Seismic Exploration*, 32: 479-506.

The ill-posed nature of geophysical problems requires the incorporation of an appropriate regularization function into the associated optimization framework. Usually, the choice of the regularization function depends on prior information about the properties of the unknown model parameters. As a conventional regularization function, Tikhonov regularization fails when reconstructing models with sharp discontinuities. In contrast, the first-order total variation regularization (TV) can reconstruct sharp edges or models with block-like features. Neither of these regularizations can reconstruct models with complex geometry that has both smooth and blocky features. In this study, we investigate different regularization functions for nonlinear seismic travel-time (cross-hole) tomography, where the model parameter is slowness. We use the alternating direction method of multipliers (ADMM) to solve the optimization with TV regularization. Also, a balanced combination of Tikhonov-TV regularizations in either its conventional form or new version with automatic balancing parameter is proposed for the nonlinear travelttime inversion. Using synthetic examples, we first show the robustness of the TV regularization solved by ADMM and also the good performance of the Tikhonov-TV regularization in recovering models with smooth blocky structures.

**KEY WORDS:** nonlinear travel-time tomography, Tikhonov-regularization, total variation, alternating direction method of multipliers.

## INTRODUCTION

Seismic travel-time inversion (or tomography) is considered one of the conventional methods for building velocity models, the results of which can be used for seismic migration purposes or as initial models for advanced inversion techniques such as full waveform inversion (Virieux and Operto, 2009). The concern of this study is kinematic transmission tomography, which is inherently nonlinear, and the associated problem is challenging (Rawlinson and Sambridge, 2003). The travel-time tomography can be posed as an optimization problem in which the goal is to estimate unknown model parameters (e.g., velocity) by defining an objective function based on the data misfit error (e.g., least squares metric) (Sebudandi and Toint, 1993). Similar to the various geophysical problems, travel time inversion is a non-unique and ill-posed problem (Gholami and Siahkoochi, 2010). Regularization is a tool to deal with the ill-posedness problem by adding a set of constraints (or regularization functions) to the objective function. In this way, some prior information about the model is included in the problem formulation resulting in reducing the degree of non-uniqueness (Hansen, 1998, Kabanikhin, 2008; Aster, 2018) can be imposed. A simple way to deal with the ill-posedness of the problem and the poor conditioning of the Hessian operator is to add a positive value to the main diagonal of the Hessian of the least squares solution. From a mathematical point of view, this is equivalent to increasing the eigenvalues of the operator by the same amount. In this way, the problem is more tractable. The optimization for this case is called damped least squares or zero-order Tikhonov regularization.

Another simple and classical regularization approach is to bias the model toward smooth behavior using an L2 norm-based regularization function or Tikhonov regularization (Tikhonov and Arsenin, 1977). However, Tikhonov regularization blurs the sharp discontinuities due to the short-tailed nature of the Gaussian distribution (Gheymasi et al., 2016). Another class of the regularization approaches is based on the L1 norm (or a semi-norm) of the solution and induces sparsity in the solution (e.g., Rudin et al., 1992; Figueiredo et al., 2007; Goldstein and Osher, 2009). Total variation regularization (TV) (Rudin et al., 1992), based on the blockiness assumption, has become an important tool in image processing (e.g., Chartrand and Wohlberg, 2010) or seismic applications (e.g., Aghamiry et al., 2019a; Liu et al., 2021). Unlike the Tikhonov regularization, TV regularization is an edge-preserving method and can be used for parameter estimation problems with discontinuities. Promoting sparsity with regard to a single higher-order derivative of the model is usually undesirable; for example, TV2 (second-order TV regularization) encourages piecewise linear solutions. However, combinations of different model derivatives have recently piqued the interest of researchers, and the higher-order total variation, as well as the original first-order variation, serve as the foundation of such techniques (Stefan et al., 2010; Benning et al., 2013).

Total Generalized Variation (TGV) regularization, also known as second-order Total Generalized Variation (TGV), has been applied to Magnetic Resonance Imaging (MRI), which aims at reconstructing both smooth and blocky features of the model with a good degree of accuracy (Gong et al., 2018). TGV regularization has also been used in EIT reconstruction, in which it creates more realistic images than TV regularization (Gong et al., 2018).

From a statistical perspective, different statistical properties of smooth and sharp media impede individual regularizations to recover both smooth and sharp features simultaneously. Gholami and Hosseini (2013) proposed a novel approach that considers both Tikhonov and TV regularizations in a balanced framework to reconstruct piecewise smooth models (piecewise constant models embedded in a smooth background). In their work, the model in the optimization problem is divided into two terms, one for smooth behavior and another for piecewise constant features. Then, a suitable regularization function (second-order Tikhonov and first-order TV) is considered for each term. This new regularization function can handle the blurriness imprint of Tikhonov and the staircase imprint of TV.

In this study, we focus on the regularization of nonlinear traveltime tomography, evaluating Tikhonov, TV, and their balanced combination (Tikhonov-TV). To apply the regularization, the original nonlinear problem is transformed into a locally linear problem by taking advantage of Occam's inversion (Constable et al., 1987). To deal with the non-differentiability of the TV-norm, we take advantage of the alternating direction method of multipliers (ADMM) (Boyd, 2010), which replaces the constrained optimization associated with the TV-norm with the corresponding augmented Lagrangian function. Then, ADMM decomposes the original problem into easy-to-handle subproblems. Other methods for tackling constraint optimization problems, such as the L1 norm, can also be utilized. For example, the split Bregman approach (Goldstein and Osher, 2009) is equal to ADMM for basis pursuit and related issues. The types of problems that ADMM and split Bregman can tackle are fundamentally different. ADMM can be used to solve a wide range of problems, including ones with linear constraints. Split Bregman, on the other hand, is especially effective for problems involving the minimization of the sum of two convex functions, one of which is an L1 norm (Boyd, 2010).

We use the ADMM method for solving the least squares problem involving either TV or Tikhonov-TV regularizations. Regularized nonlinear travel time tomography is studied for different scenarios. In the following, we first give a brief explanation of the different regularization functions and then investigate their performance in the numerical sections using synthetic experiments.

## METHOD AND THEORY

In this section, we briefly explain the regularization method in seismic tomography. In seismic tomography, the goal is to reconstruct the medium parameter using recorded seismic waveforms (e.g., first arrival times). The associated optimization procedure is iterative, and in each iteration, we compute the seismic response to update the model parameter. In travel-time tomography, the travel-time data is calculated as (Sambridge and Kennett, 1990):

(1)

where  $L$  is the path of the ray generated from the source to the receiver, and the integration path depends on  $v$ , the velocity of the medium. The relation in (1) is a nonlinear equation and its solution is derived in the frame of the eikonal equation (Aki and Richards, 1980):

(2)

where  $T$  is the travelttime function or phase factor. There are several methods for solving the corresponding eikonal equation such as finite difference-based methods (Vidale, 1988; Hole and Zelt, 1995; Buks and Kastner, 2004). In this study, we implemented the Fast Marching Method (FMM) (Sethian, 1996, 1999; Sethian and Popovici, 1999), which is a numerical method for solving the boundary value problem of the eikonal equation. In this method, the medium is discretized, and a fixed velocity value is assigned for each grid (discrete point in the model) based on an upwind finite difference approximation of the gradient, in which the algorithm complexity (how long an algorithm would take to complete given an input of size  $N$ ) is  $O(N \log N)$ , where  $N$  denotes the number of the grids in the model (see Sethian, 1999, for a detailed review). Suppose we have a forward modeling kernel operator  $\mathcal{K}$  that computes the synthetic data (first arrival time) given the unknown model parameters,  $\mathbf{m}$ . Now, given the observed data,  $\mathbf{d}$ , the problem can be put into a compact algebraic form describing a nonlinear system of equations:

(3)

Due to the high scale of geophysical applications, eq. (3) is outlined in the context of local optimization, where the initial model is iteratively refined to minimize a predefined criterion called the cost function. The optimal solution is then the minimizer of the cost function.

The success of local optimization depends on how close the initial model is to the optimal solution (Nocedal and Wright, 2006). The use of regularization in optimization is well-documented for linear problems. Here we are dealing with non-linear travel-time tomography. For a simple implementation of regularization, one can take advantage of Occam's inversion for nonlinear problems. Occam's inversion involves a local linearization of the problem during iterations using the Taylor expansion (Constable et al., 1987):

$$\mathbf{J}^T \mathbf{J} \mathbf{m} = \mathbf{J}^T \mathbf{d}, \quad (4)$$

where  $\mathbf{J}$  is the Jacobian matrix that describes the sensitivity of modeled data to the model parameters and  $\mathbf{m}$  denotes the model perturbation. By substituting eq. (4) into eq. (3) we have:

$$\mathbf{J}^T \mathbf{J} \mathbf{m} = \mathbf{J}^T \mathbf{d} - \mathbf{J}^T \mathbf{J} \mathbf{m}_0. \quad (5)$$

Now, we have a linear equation concerning  $\mathbf{m}$ . Note that  $\mathbf{J}^T \mathbf{J}$  and we have:

$$\mathbf{J}^T \mathbf{J} \mathbf{m} = \mathbf{J}^T \mathbf{d} - \mathbf{J}^T \mathbf{J} \mathbf{m}_0. \quad (6)$$

$$\mathbf{J}^T \mathbf{J} \mathbf{m} = \mathbf{J}^T \mathbf{d} - \mathbf{J}^T \mathbf{J} \mathbf{m}_0. \quad (7)$$

We can see that  $\mathbf{J}^T \mathbf{J}$  is linear concerning  $\mathbf{m}$ . In what follows we use  $\mathbf{J}^T \mathbf{J}$  and to have a consistent notation with linear inverse problem literature.

Note that in eq. (1), when the structure of the operator  $\mathbf{J}$  is independent of the model parameters in the current iteration ( $k$ ), we have a linear travel-time inversion. In the Tikhonov regularization, the desired model we seek has the smallest seminorm as  $\|\mathbf{m}\|$ , where  $\mathbf{D}$  is a finite difference operator and  $\|\cdot\|$  is the L2 norm (or Euclidean norm):

$$\mathbf{J}^T \mathbf{J} \mathbf{m} = \mathbf{J}^T \mathbf{d} - \mathbf{J}^T \mathbf{J} \mathbf{m}_0 + \lambda \mathbf{D}^T \mathbf{D} \mathbf{m}. \quad (8)$$

where  $\lambda$  is the regularization parameter that controls the tradeoff between the data misfit term and the model regularization term. A high value of  $\lambda$  gives more weight to the model term and vice versa. Problem (8) is known as Tikhonov regularization (Tikhonov and Arsenin, 1977) or damped least squares (for  $\mathbf{D}$  identity matrix). Tikhonov regularization deals with models

containing mainly smooth features and is popular because of its simple and straightforward implementation (Hansen, 1998).

### *Total Variation regularization*

In total variation regularization, we seek a solution with a certain structural shape (i.e., piece-wise). The Optimization with TV functional is encapsulated by the following formulation (Rudin et al., 1992; Goldstein and Osher, 2009):

(9)

which uses the L1-norm of the model gradient as a regularization term, where  $\mathbf{A}$  is arbitrary linear transformation matrix (finite difference operator) and  $\mathcal{C}$  is a convex set bounded by upper and lower values of  $\mathbf{y}$ : (Maharramov and Levin, 2015; Aghamiry et al., 2019):

(10)

Problem (9) is also referred to as a generalized lasso (Boyd et al., 2011, Tibshirani and Taylor, 2011), in which the goal is to find an optimal vector of model parameters by promoting blocking through either an isotropic or anisotropic TV norm and fitting the data in the least squares sense. In the isotropic sense, the TV function reads:

(11)

where  $\mathbf{D}_x$  and  $\mathbf{D}_z$  are the first-order difference operator in the x-and z directions, respectively. The objective function in (9) is non-differentiable and its solution can be obtained using, for example, iteratively reweighted least squares (IRLS) (Scales et al., 1988), Split-Bregman (Goldstein and Osher, 2009) or ADMM (Wahlberg et al., 2012).

### *Balanced Tikhonov-TV regularization*

In balanced Tikhonov-TV regularization, the following regularization function has been proposed (Gholami and Hosseini, 2013; Aghamiry et al., 2019b):

$$, \tag{12}$$

where  $\Delta_x$  and  $\Delta_y$  are first and second-order finite difference operators, respectively. Note that the regularization function in (12) is a balanced combination of semi-L2 and L1 norms, where the constant value  $\alpha$  determines how much the regularization function weights each part. We assume here that model  $m$  is a combination of two features; one with smooth behavior  $m_s$  and the second with piece-wise blocky structure  $m_b$ . Therefore, this regularization is suitable for piecewise-smooth models. Moreover, the regularization function in (12) is general, because if  $\alpha \rightarrow 0$ , Tikhonov regularization is obtained and  $\alpha \rightarrow \infty$  leads to the TV -regularization. The objective function of Tikhonov-TV regularization in eq.(12) can be efficiently solved by ADMM (see the Appendix).

## NUMERICAL EXAMPLES

With the vector of first arrival times as the observation data, the first step in travel-time tomography in the context of nonlinear inversion is to construct the forward operator that solves the travel-time equation. Unlike linear travel-time tomography, where the operator depends only on the source-receiver geometry, in nonlinear inversion, the input to this operator is the vector of model parameters in the predefined grids (or meshes) and source-receiver geometry. While in linear travel-time tomography, we are dealing with the linear path of the rays from the source to the receivers regardless of the properties of the medium, in nonlinear ray-based tomography the ray path changes in the presence of an anomaly. For example, for the synthetic model shown in Fig. 1, we performed ray tracing with 21 sources (left hole) and 21 receivers (right hole). Note that for all models shown in the following the unit of colorbars is m/s. The rays generated by the sources are interested to go through an anomaly with higher velocity  $v_2$  (Fig. 2).

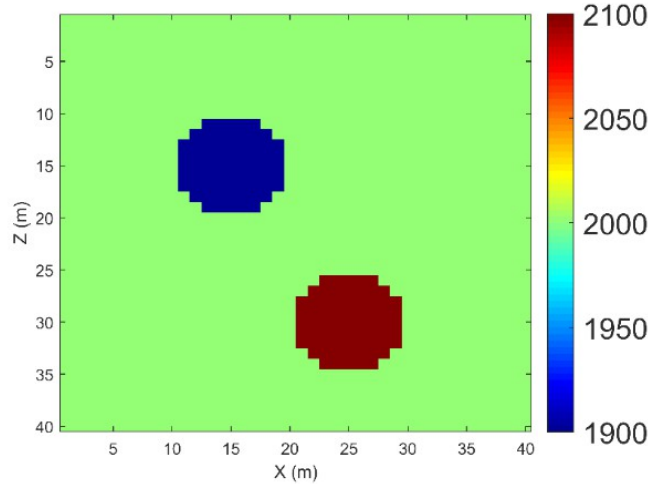
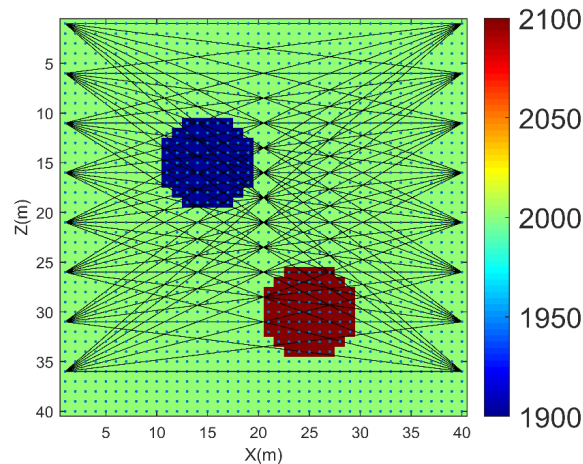


Fig. 1. Synthetic 2D velocity model.

It is worth mentioning that we usually look for anomalies in the real medium. The presence of such anomalies changes the ray path and consequently the arrival times. Fig. 3 compares to the modeling shown in Fig. 2. The difference in travel time difference between the linear and nonlinear modeling can be seen. It is important to simulate the real world, otherwise, such differences will have a negative effect as noise. However, performing linear tomography is more manageable than the nonlinear case. A comparison between the inversion results of linear data using linear tomography and nonlinear data using nonlinear inversion tomography is given in Fig. 4, which highlights a better image obtained by linear tomography. The linear and nonlinear inversion problem is solved using Occam and Gauss-Newton methods, respectively.





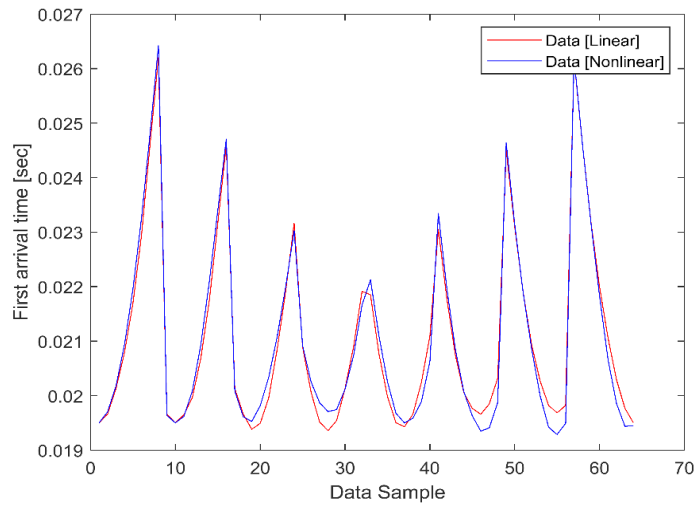
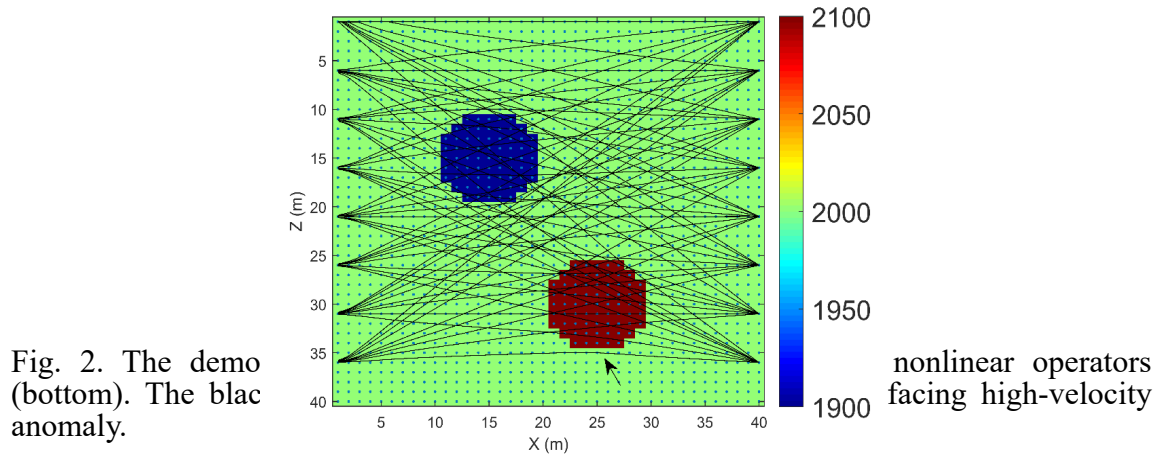


Fig. 3. Comparison between first arrival times obtained by linear modeling (red curve) and nonlinear modeling (blue curve).

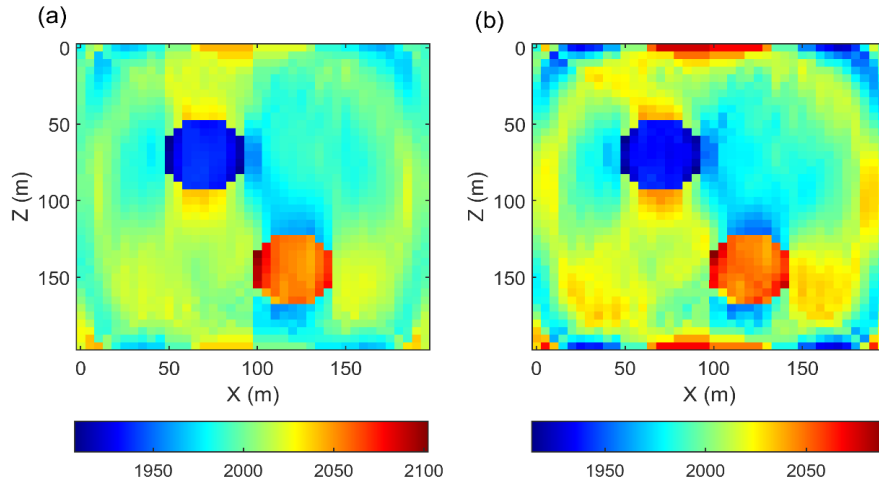


Fig. 4. Comparison between the inversion results of linear (a) and nonlinear inversion tomography (b).

### *Tikhonov Regularization*

For the synthetic model shown in Fig. 1 and for the observed data shown in Fig. 3 (nonlinear case), we performed Occam's inversion using Tikhonov regularization. One can use a fixed damping constant for all iterations. However, the problem is still nonlinear and it is recommended to start the inversion with a high value of the damping constant and gradually decrease it so that at the convergence point the value approaches zero. One approach to set the damping constant (or regularization parameter) can be as (Gholami and Siahkoobi, 2010):

$$(13)$$

Here,  $\alpha_k$  is the value of the regularization parameter at the  $k^{\text{th}}$  iteration, and  $\alpha_{k+1}$  is the current estimate using proposed methods such as the discrepancy principle (Morozov, 1984) or simply based on a percentage of the main diagonal of the Hessian matrix ( $H_k$ ). The most appropriate value of the regularization parameter that strikes an appropriate balance between the data misfit term and the regularization part is difficult to achieve in practice, and the situation becomes even more difficult in the case of nonlinear

inversion. In this study, we evaluate different algorithms based on initialization with different regularization parameters and adjust their value during iteration based on the recipe given in (13).

It is worth noting that the condition number of  $\mathbf{A}$  for this example is of order  $10^6$ , indicating a high degree of ill-posedness of the original problem. Thus, the simple least squares optimization fails. We start the inversion with the background model as the initial model. Although, one can cope with the ill-conditioning of the problem using the damped least squares approach, however, an important step is to enforce some prior knowledge about the unknown model parameters.

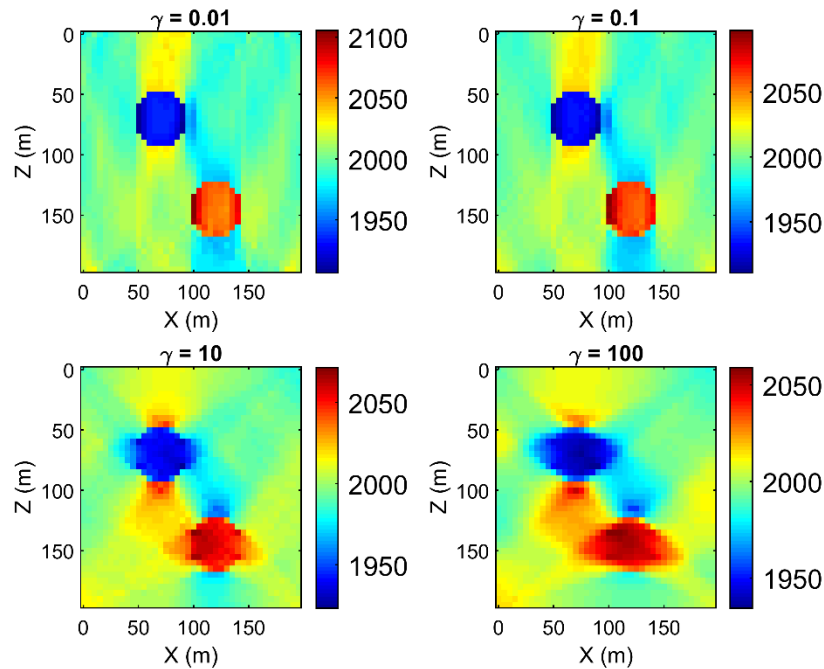


Fig. 5. Reconstructed models obtained by Tikhonov regularization with different initialization of  $\mathbf{m}_0$ .

As one of the most commonly used regularization methods, Tikhonov regularization is performed with a different regularization parameter ( $\gamma$ ), and the results are shown in Fig. 5. From Fig. 5, it can be seen that the Tikhonov regularization was able to reconstruct the parts of the model located in the null space of the problem, in particular for  $\gamma = 10$ . We used a first-order Tikhonov operator here. However, depending on the problem and subsurface characteristics, a higher-order finite difference operator may also be used.

### *Total Variation Regularization*

Next, TV regularization is assessed for this example. Here TV-regularized objective function is optimized using two approaches: IRLS and ADMM. Similar to the previous experiment, the inversion is performed with  $\lambda$ . The ADMM method is performed within 30 iterations. The penalty parameters are determined based on trial and error and due to the insensitivity of ADMM iteration to the penalty parameter(s) a fixed set of parameters can be used during the iterations (Nocedal and Wright, 2006). The TV regularization results solved by the ADMM method are shown in Fig. 6. It can be seen that for  $\lambda$  a nearly perfect reconstruction of the model is achieved. Furthermore, for the case of  $\lambda$ , a significant improvement of the model update is obtained compared to the first-order Tikhonov regularization (Fig. 5). For a detailed comparison, we extracted the diagonal logs (main diagonal of the 2D models) for different  $\lambda$ , and the results are shown in Fig. 7 that demonstrate a perfect agreement of the estimated models (blue line) with the true model (red line) for.

There are various methods to tackle the non-differentiability of TV norms such as the fast iterative soft thresholding algorithm (FISTA) (Beck and Teboulle, 2009). Perhaps the most used method is IRLS (Aster, 2018) which addresses the problem by solving a sequence of weighted least squares problems via a diagonal weighting matrix as

in the left-hand side of the normal equation related to Occam's inversion:

$$\cdot \quad (14)$$

Starting from  $\lambda$ , the values of  $\lambda$  are updated iteratively until a good convergence point. We performed the inversion with IRLS as well and its comparison with ADMM is shown in Fig. 8).

Here we have initialized the inversion with  $\lambda$ . Figs. 8a and 8b are the reconstructed models obtained with IRLS and ADMM, respectively, in which a better reconstruction of the model is obtained by the ADMM approach. Also, in Fig. 8c, the model error (the difference between the true model and the estimated model) is shown in terms of least squares as a function of iteration number, indicating a better convergence rate of ADMM for this example. One can obtain better results with IRLS. However, in this example, an identical experiment (and inversion) configuration is used.

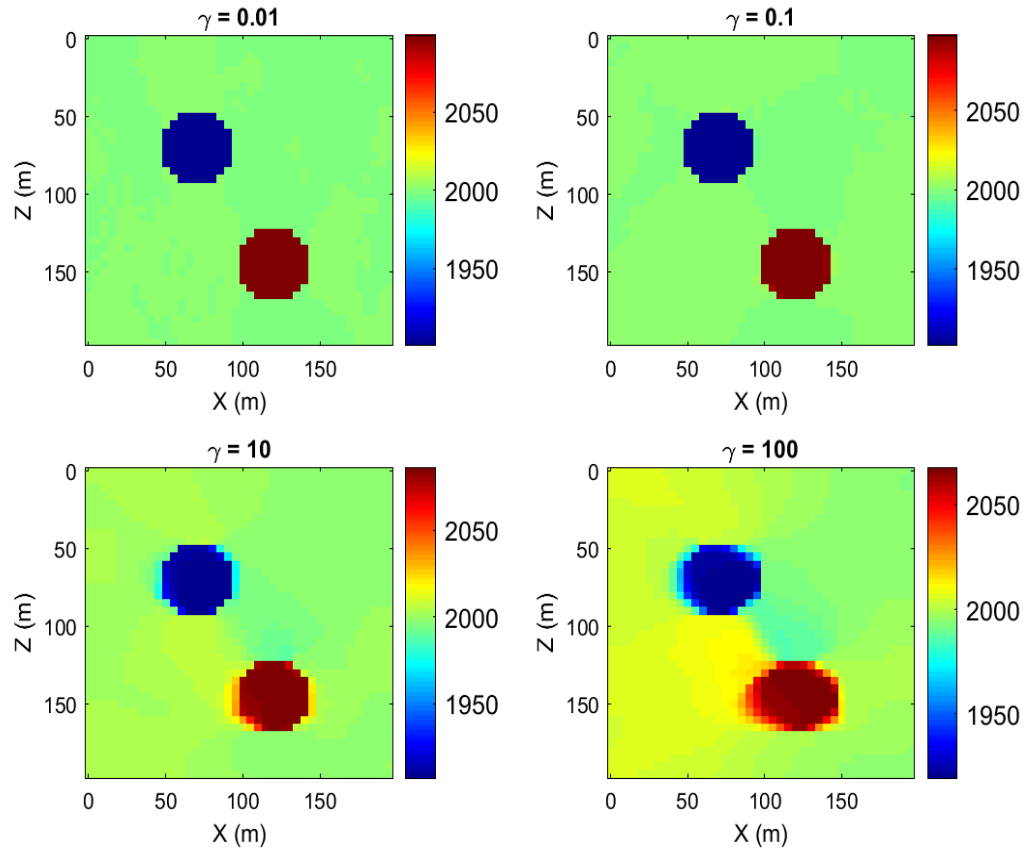


Fig. 6. Nonlinear tomography results using TV regularization solved by the ADMM approach. Each figure is related to specific initialization.

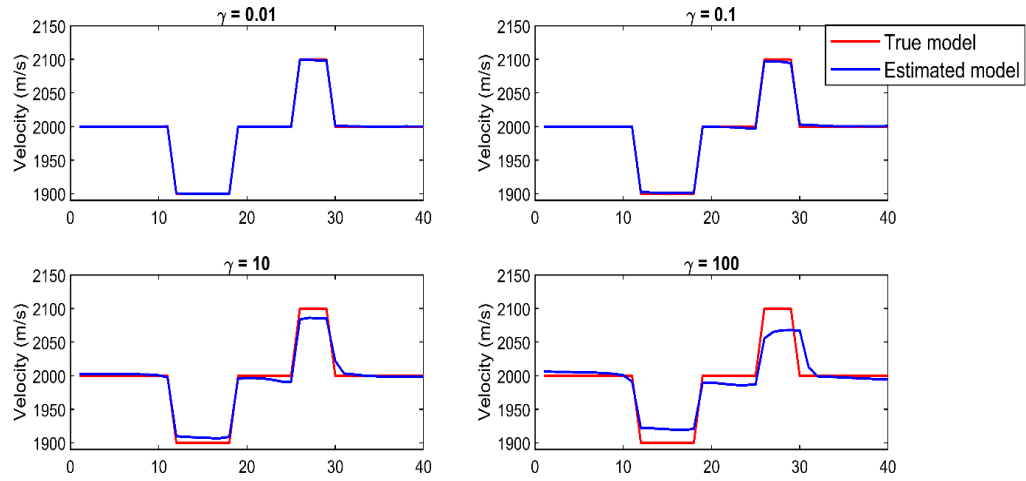


Fig. 7. Extracted log (diagonal of the original) matrix for the true model (red line) and estimated model (from Fig. 6) (blue line).

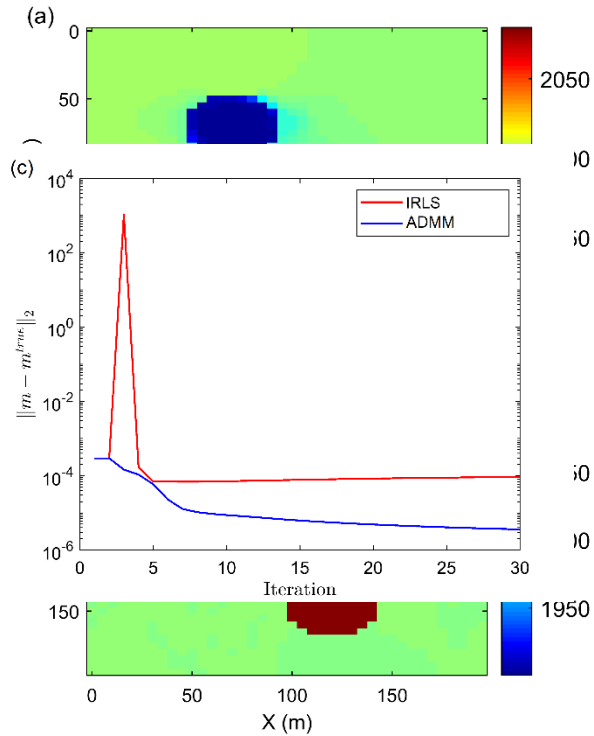


Fig. 8. Nonlinear tomography results with TV regularization solved by (a) IRLS and (b) ADMM with initialization. (c) L2 norm of model error (error between true and estimated model) versus iteration number.

### *TV regularization for sparse acquisition*

In geophysical applications, we usually deal with environments that are difficult to access. For example, harsh terrain or environmental constraints and the high cost of data acquisition make dense (or regular) data collection difficult. As a result, insufficient data may be available. From an optimization perspective, the size of the data space decreases relative to the model space. Therefore, it is more difficult to handle underdetermined systems of equations. From a physical point of view, decreasing the number of source-receiver pairs means insufficient ray coverage, which can increase the null space of the model. For example, Fig. (9) compares two different cases of coverage: one with dense source-receiver spacing and one with only three sources (sparse acquisition). A significant difference in the ray coverage and some regions of the sparse acquisition case can be seen. One of the applications of L1 norm-based regularizations is dealing with sparse settings (Aghamiry et al., 2020). Such problems can be studied using compressive sensing. Here, we are concerned

with the reconstruction of models in the presence of an insufficient recording. An experiment is conducted to analyze the performance of TV regularization in such scenarios. The results are summarized in Fig. 10 for different numbers of sources ( $S$ ) and receivers ( $R$ ). The quality of the inverted model decreases when we reduce the number of sources and also receivers (which means less ray coverage). However, with a number of 3 sources and 11 receivers, the TV-regularized nonlinear tomography gives satisfactory results.

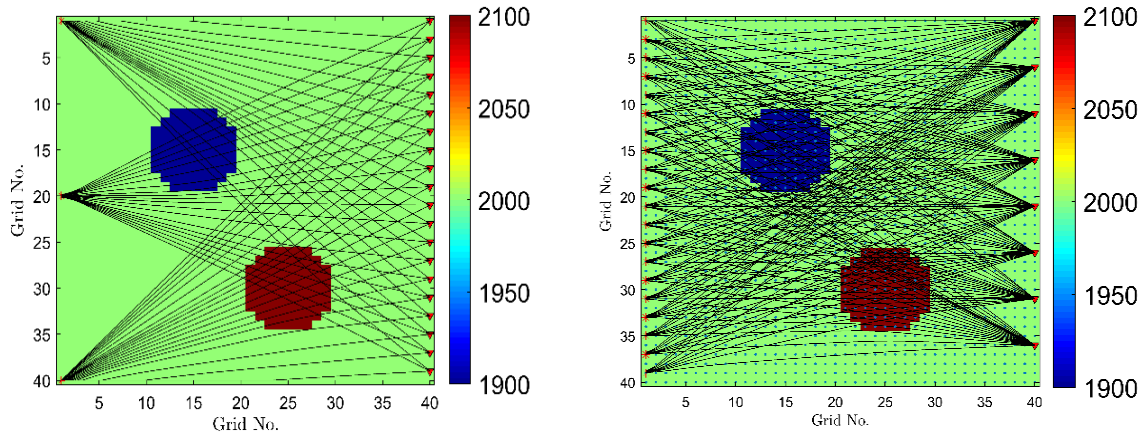


Fig. 9. Comparison between the ray coverage via dense acquisition (left) and sparse acquisition (right).



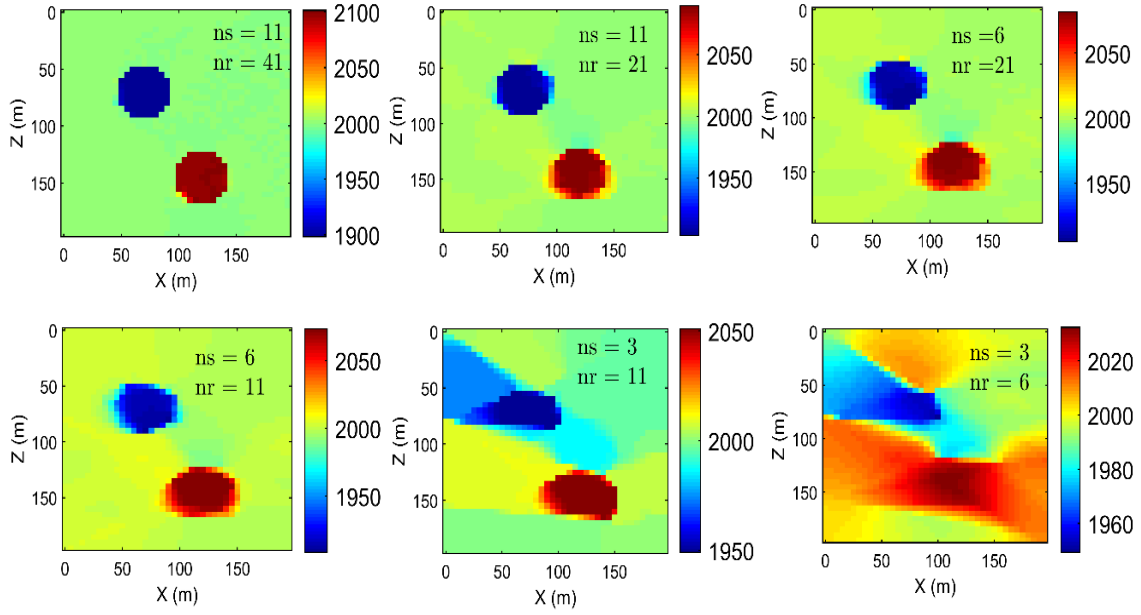


Fig. 10. The reconstructed model obtained by TV-regularized nonlinear tomography for sparse acquisition experiment. The number of sources and receivers are labeled by  $ns$  and  $nr$ , respectively.

Table 1 gathers the model error,  $\epsilon$ , for the models shown in Fig. 10.

Table 1: The calculated model error for nonlinear tomography with different source ( $ns$ )-receiver ( $nr$ ) numbers.

Error	Number of Receivers ( $nr$ )	Number of Sources ( $ns$ )
33.29	41	11
176.87	21	11
259.60	21	6
314.574	11	6
545.68	11	3

684.89	6	3
--------	---	---

### *Tikhonov-TV regularization*

#### *Model I*

We have noted that for the goal of subsurface imaging, we are interested in a general regularization function that can cover models with both smooth and blocky features. Suppose that the medium whose features we wish to estimate both smooth and blocky structures (Fig. 11). In this model, the low-velocity anomalies have smooth variation. In contrast, anomalies with high-velocity velocities contain block-like structures. The tomographic acquisition is performed with 25 sources on the left side and 25 receivers on the right side of the model. We performed nonlinear seismic tomography with Tikhonov, TV, and Tikhonov-TV regularizations. The results of the inversion are shown in Fig. 12. In Figs. 12a-c the results obtained with Tikhonov, TV, and their balanced combination via Tikhonov-TV regularization are demonstrated,

It can be seen that the Tikhonov-TV regularization outperformed the others. For example, even for blocky features, Tikhonov-TV regularization has better performance than TV regularization. Tikhonov-TV regularization was able to reconstruct both smooth and blocky features simultaneously. For a more detailed comparison, the extracted vertical logs at three locations are shown in Fig. 13. Together with the computed model error summarized in Table 2, which shows the robustness of the Tikhonov-TV regularization. This regularization incorporates the functionality of both the Tikhonov and TV regularizations and can be used for other seismic applications.

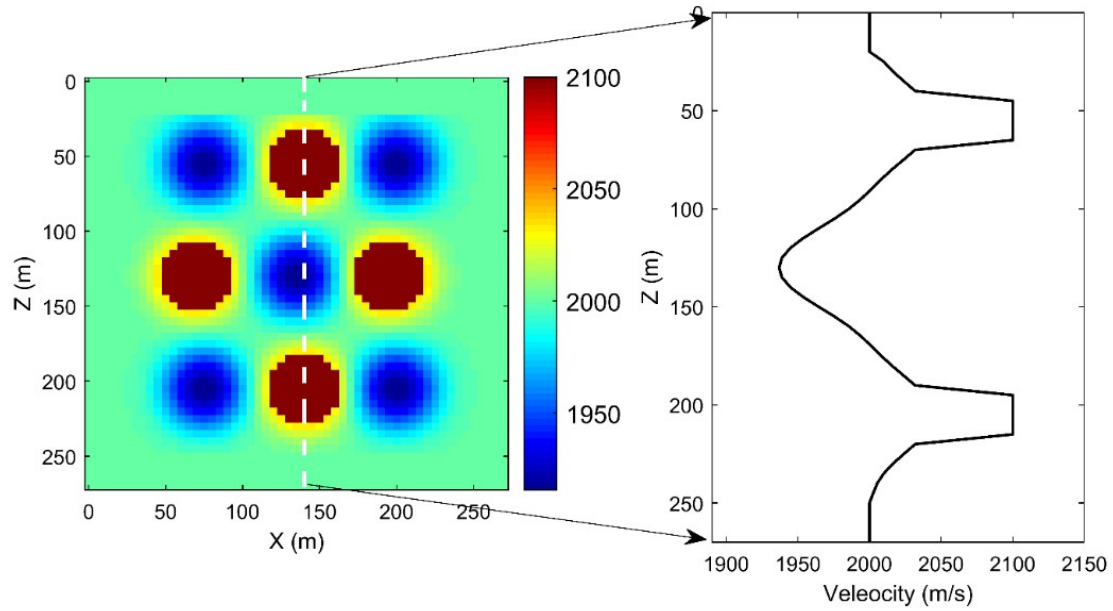


Fig. 11. Velocity model containing smooth (low-velocity) features and piece-wise (high velocity) features. The vertical log associated with white dashed line (middle of the model) is also demonstrated.

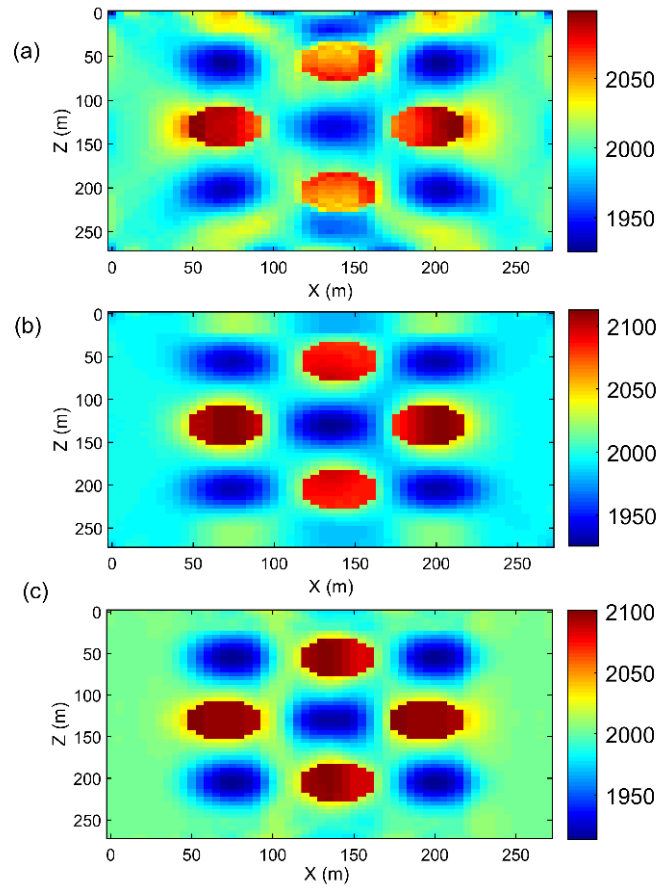


Fig. 12. Regularized nonlinear tomography results obtained by (a) Tikhonov, (b) TV and (c) Tikhonov-TV regularization.

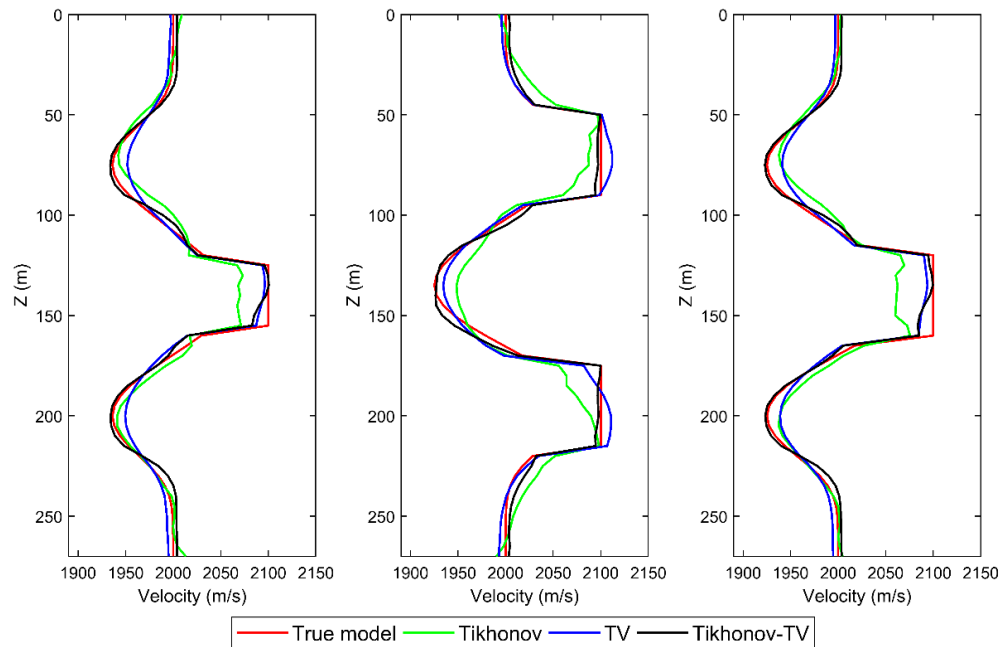


Fig. 13. Comparison between extracted vertical logs at (from left to right)

Table 2. The calculated model error for Tikhonov, TV, and Tikhonov-TV regularized nonlinear tomography.

Tikhonov-TV	TV	Tikhonov	Method
323.31	504.36	908.38	

### *Model II*

The evaluation of various regularization methods is conducted with a more realistic model (Fig. 14). A high-velocity anomaly is embedded within a smooth baseline velocity in this model. Using ray tracing, the first arrival time from the observed data is obtained (Fig. 15). The observed data are illustrated in Fig. 16. Nonlinear travel-time tomography is performed utilizing Tikhonov, TV, and Tikhonov-TV regularizations, beginning with a velocity model whose value increases linearly from 4000 to 4500 m/s. The regularization parameter is set based on trial and error. The inversion results after 30 iterations are shown in Fig. 17, with the results of Tikhonov regularization (Fig. 17a), TV regularization (Fig. 17c), and Tikhonov-TV regularization (Fig. 17e) shown in the left column. Figs. 17b, 17d, and 17f depict the difference between the true velocity model and the inversion results in the left column. On the basis of the difference plot, Tikhonov-TV regularization outperforms other regularization strategies. In this case, Tikhonov regularization fails to reconstruct the details of the model. With TV regularization, the inversion is unable to recover the high-velocity anomaly. However, from the different plots, it can be seen that Tikhonov-TV regularization successfully recovered most of the features of the model.

Some extracted velocity profiles depicted in Fig. 18 demonstrate the superiority of the Tikhonov-TV regularization, with the blue and green arrows representing the failure of the TV and Tikhonov regularizations, respectively.

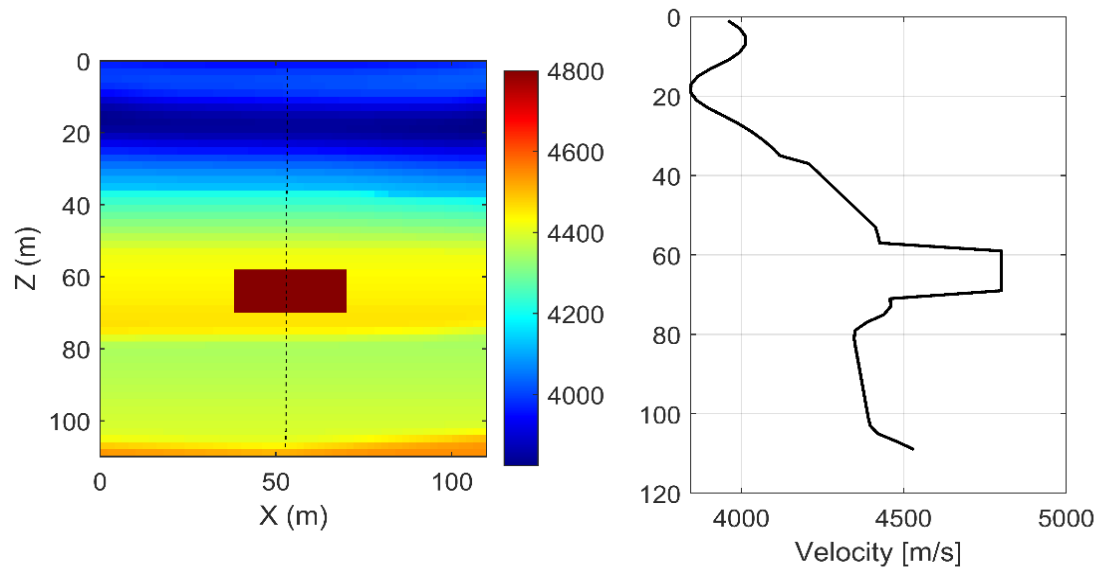


Fig. 14. Velocity model 2 and a vertical profile (related to the vertical dashed line) that includes both smooth and blocky features.

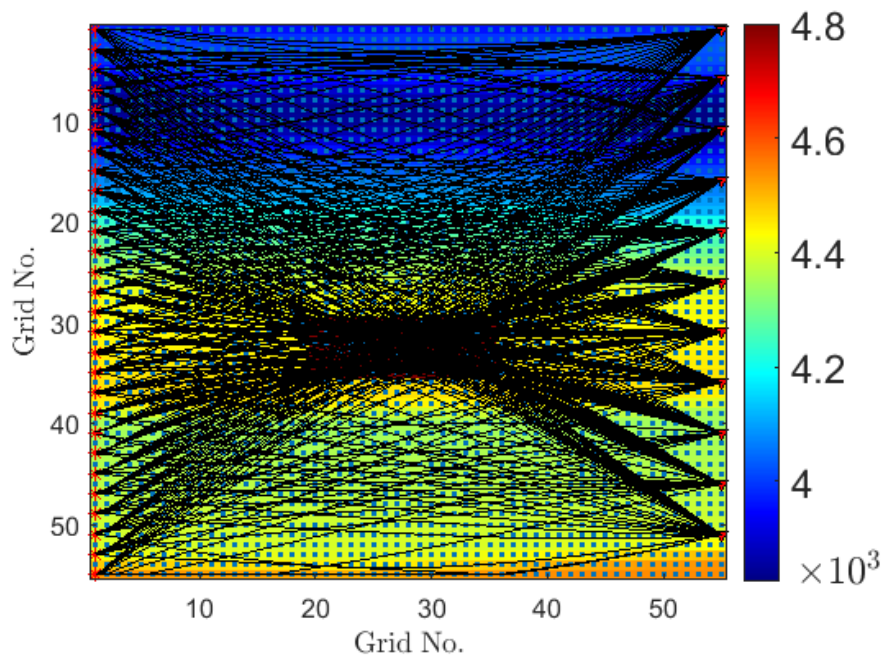


Fig. 15. The ray tracing for the velocity model is shown in Fig. 14.

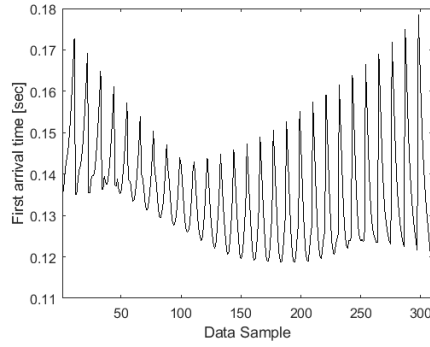


Fig.16. The first arrival time related to the ray tracing shown in Fig. 15.

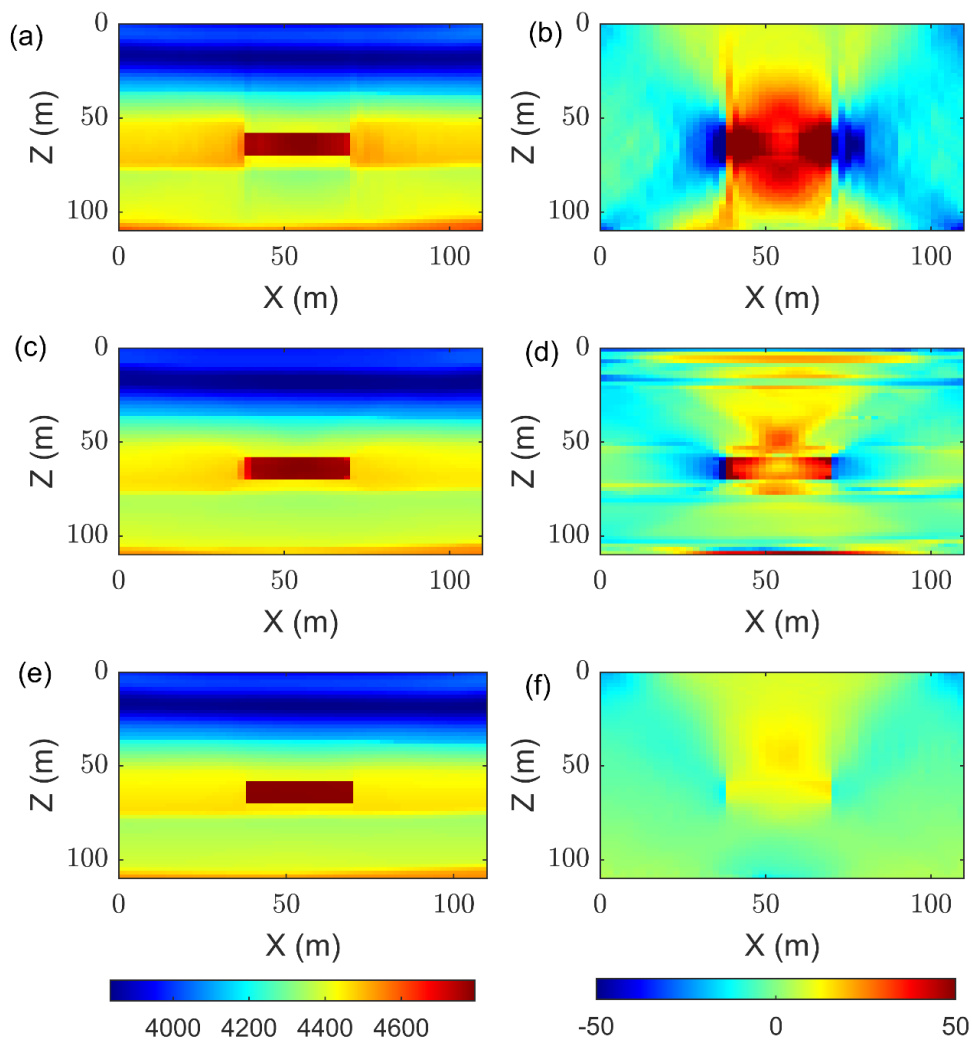


Fig. 17. Inversion results obtained by the Tikhonov regularization (a), TV regularization (c) and Tikhonov-TV regularization (e). The difference between true model and estimated model obtained by Tikhonov regularization (b), TV regularization (d) and

Tikhonov-TV regularization (f).

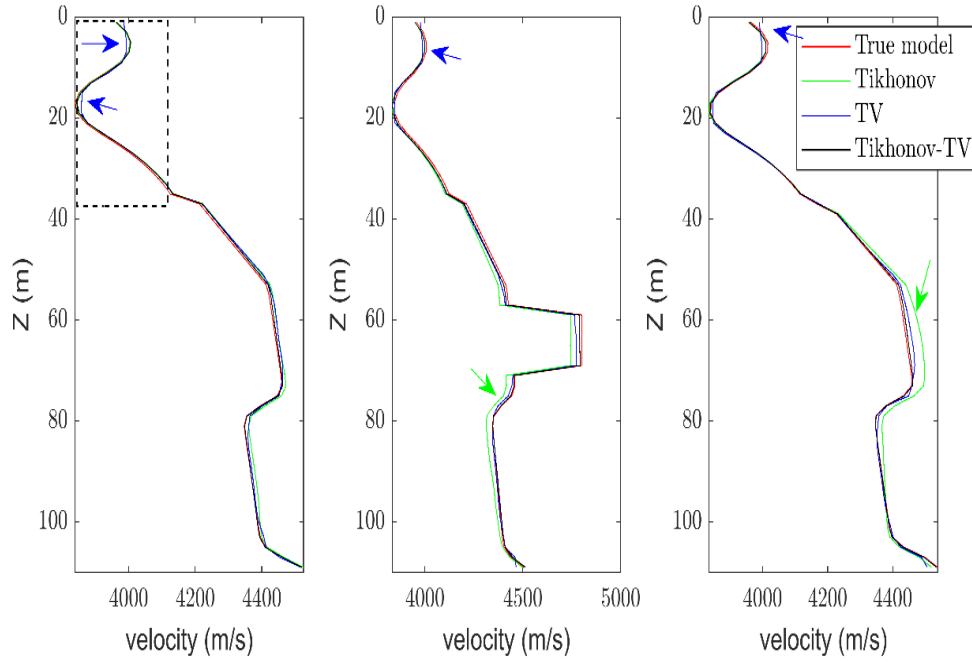


Fig. 18. Comparison between extracted velocity profiles located at from models shown in Fig. 22. Green and blue arrows show the failure of Tikhonov and TV regularizations in reconstructing the model.

Fig. 19 depicts a magnified depiction of the selected portion in the first column of Fig. 18 for comparison purposes. In addition, the least squares norm of the data misfit (the difference between calculated data using estimated velocity models during iterations) is shown in Fig. 20.



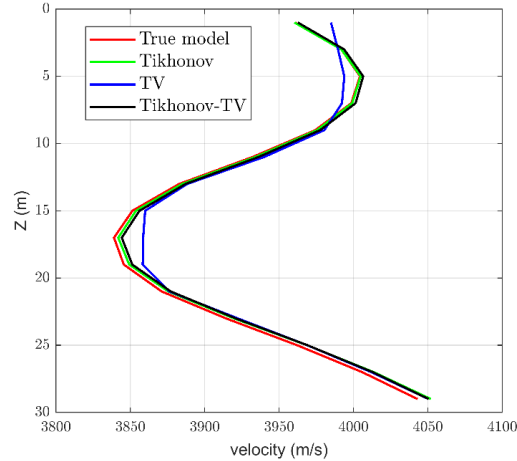


Fig. 19. Magnified image of the rectangle sketched in Fig. 18.

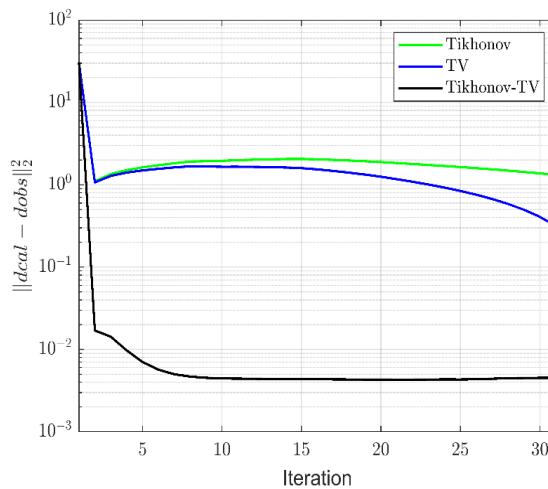


Fig. 20. The computed data misfit term versus iteration for different regularization methods.

## Noise-contaminated data

Unwanted errors, known as noise, are common in geophysical data. The calculated arrival time is the first phase of the waveforms in time-time tomography, and it is sensitive to random (Gaussian-distributed) noise or operator error during the phase-picking process. When a problem is being solved, it is sometimes unstable, which means that a slight change in the data will result in a huge change in the reconstructed model. To deal with such unwanted conditions, regularization might be used. Fig. 21 depicts the evaluation of various regularization approaches on noise-contaminated data

(Fig. 21), which has the same description as Fig. 17. According to the demonstrated inversion results, corresponding model differences, and the vertical velocity profiles shown in Fig. 23, Tikhonov regularization is unable to reconstruct the anomaly and Tikhonov-TV regularization has better performance than TV regularization.

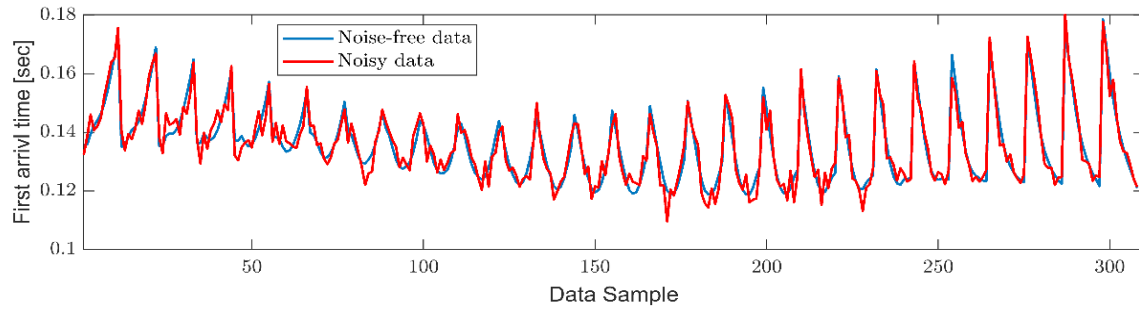


Fig. 21. Comparison between noise-free data and data contaminated by random noise.

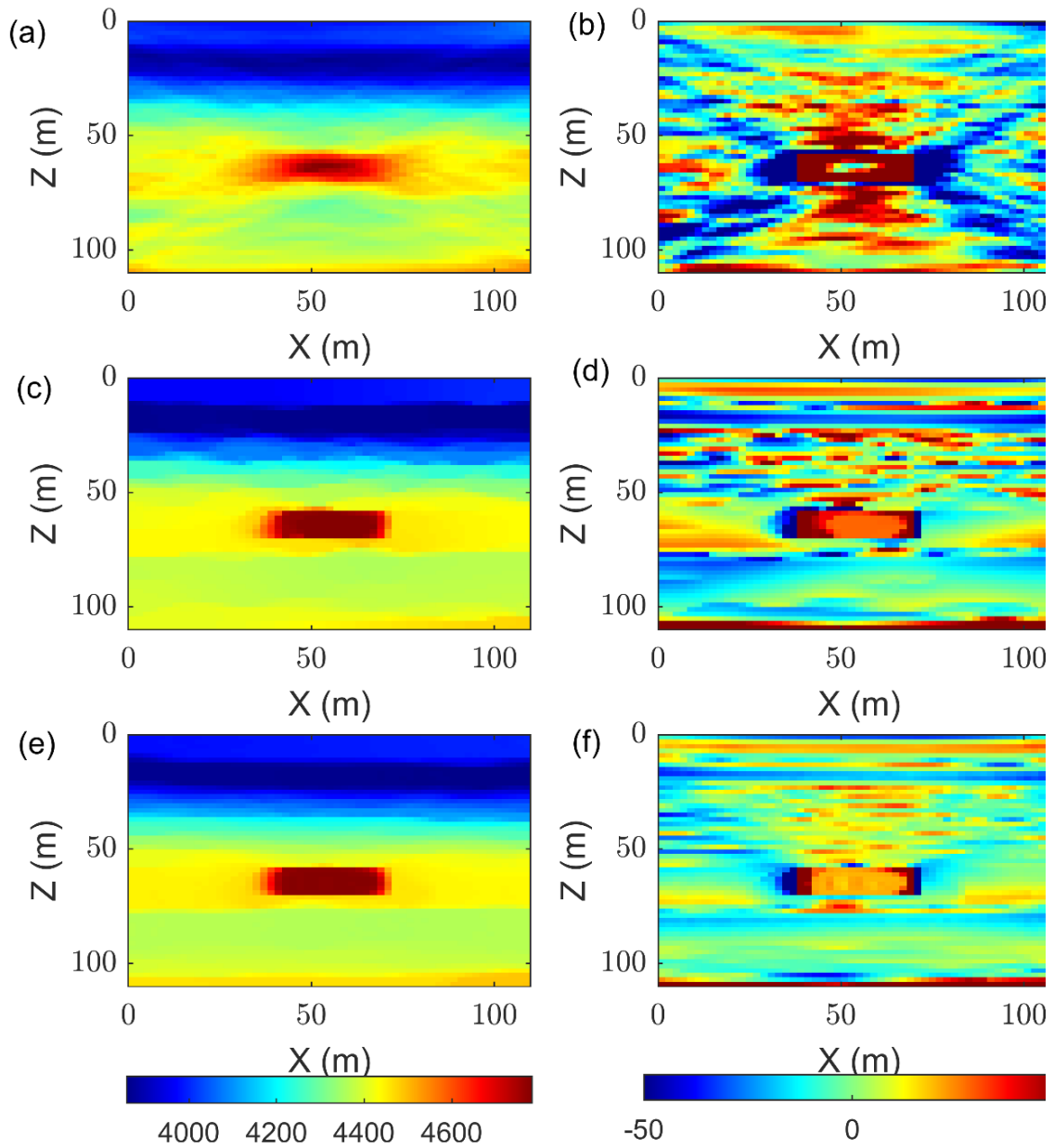


Fig. 22. Inversion results obtained by the Tikhonov regularization (a), TV regularization (c) and Tikhonov-TV regularization (e). The difference between true model and estimated model obtained by Tikhonov regularization (b), TV regularization (d) and Tikhonov-TV regularization (f).

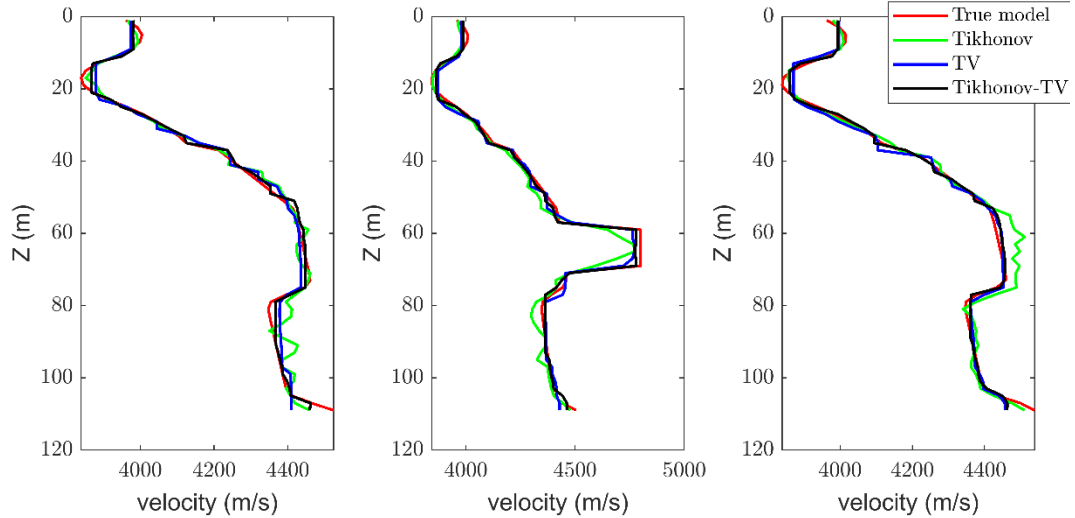


Fig. 23. Comparison between extracted velocity profiles located at from models shown in Fig. 22.

### Tikhonov-TV regularization with automatic balancing parameter

The balancing parameter ( $\alpha$ ), which defines how much the regularization function weights each segment, is an important component of Tikhonov-TV regularization. This weight was set at  $\alpha = 0.6$  in our experiments. However, this user-determined value necessitates prior knowledge of the model's structure, which is a tough undertaking. Gholami and Gazzola (2022) provided a novel way to automatically determine the value of  $\alpha$  during iterations based on robust statistics. The concept is based on considering in eq. (11) as outliers (non-Gaussian components) in the model gradient and determining in a method that distinguishes between Gaussian and non-Gaussian components. The robust z-score is used to find outliers. Gholami and Gazzola (2022) provide a full explanation of this strategy for interested readers. This new strategy is investigated, and the inversion result is given alongside the conventional approach in Figure (24), where the difference plot and data misfit error support the effectiveness of this novel regularization approach.

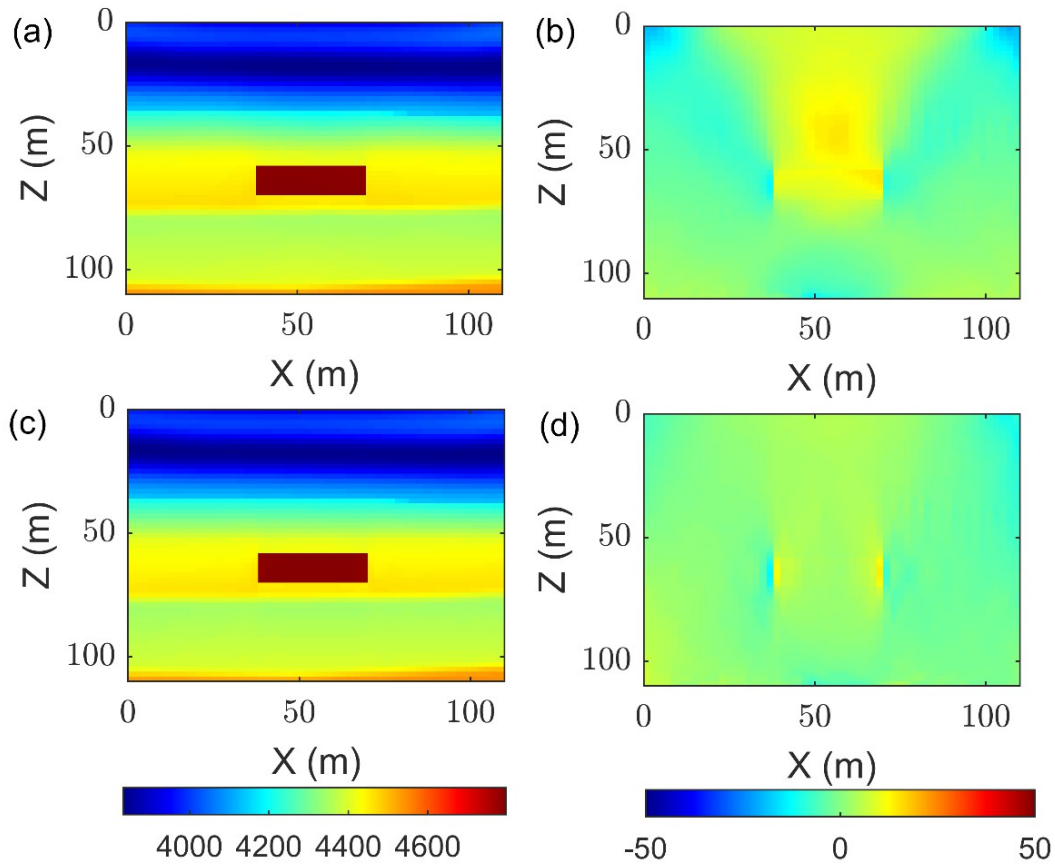


Fig. 24. Inversion results obtained by the conventional Tikhonov-TV regularization (a) and Tikhonov-TV regularization using automatic balancing parameter (c). The difference between true model and estimated model obtained by the conventional Tikhonov-TV regularization (b) and Tikhonov-TV regularization using automatic balancing parameter (d).

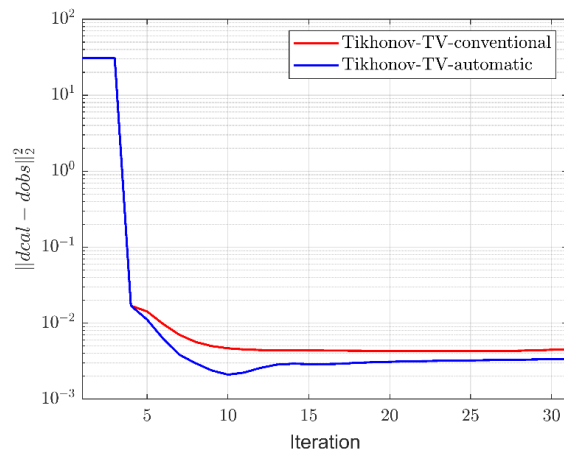


Fig. 25. The computed data misfit term versus iteration for conventional Tikhonov-TV regularization (red) and Tikhonov-TV regularization using automatic balancing

parameter (blue).

## CONCLUSION

The current study focused on the regularization of nonlinear travel-time tomography. We used Occam's inversion and replaced the nonlinear problem with a locally linear problem that allows us to use any proposed regularization function. The first option was the Tikhonov regularization. This regularization solves the ill-posedness of the problem. However, in terms of accuracy, we observed that the TV regularization yields models with high resolution. In the case of sparse data acquisition, we examined the performance of TV regularization. Next, we move to the recently developed Tikhonov-TV regularization. We perform a synthetic experiment with a synthetic model containing smooth and blocky features. We have shown that the Tikhonov-TV regularization performs well in reconstructing such models. These synthetic experiments demonstrate the superiority of the Tikhonov-TV regularization, which can be used not only for travel-time tomography but also for many geophysical applications concerned with imaging the physical properties of the subsurface. The Tikhonov-TV regularization with the novel determination of the balancing parameter is analyzed for the case of nonlinear seismic travel-time tomography, which shows great potential for use in real-data applications. Future analysis will focus on finding the undiscovered challenges of regularization functions such as Tikhonov-TV regularization for real data sets.

## Conflict of Interest

On behalf of all authors, the corresponding author states that there is no conflict of interest.

## REFERENCES

- Aghamiry, H.S., Gholami, A. and Operto, S., 2019a. Implementing bound constraints and total-variation regularization in extended full-waveform inversion with the alternating direction method of multiplier: Application to large contrast media. *Geophys. J. Internat.*, 218; 855-872.
- Aghamiry, H.S., Gholami, A. and Operto, S., 2019b. Compound regularization of full-waveform inversion for imaging piecewise media. *IEEE Transact. Geosci. Remote Sens.*, 58: 1192-1204.
- Aghamiry, H., Gholami, A. and Operto, S., 2020. Robust Full Waveform Inversion for sparse ultra-long offset OBN data. *EAGE Seabed Seismic Today: from Acquisition to Application: 1-5*.
- Aki, K. and Richards, P.G., 1980. *Quantitative Seismology: Theory and Methods*. W.H. Freeman, San Francisco.
- Aster, R.C., Borchers, B. and Thurber, C.H., 2018. *Parameter estimation and inverse problems*. Elsevier Science Publishers, Amsterdam.
- Beck, A. and Teboulle, M., 2009. A fast iterative shrinkage-thresholding algorithm for linear inverse problems. *SIAM J. Imaging Sci.*, 2: 183-202.
- Benning, M., Brune, C., Burger, M. and Müller, J., 2013. Higher-order TV methods - enhancement via Bregman iteration. *J. Sci. Comput.*, 54: 269-310.
- Boyd, S., Parikh, N., Chu, E., Peleato, B. and Eckstein, J., 2010. Distributed optimization and statistical learning via the alternating direction method of multipliers. *Foundat. Trends Mach. Learn.*, 3: 1-122.
- Buske, S., and Kastner, U., 2004. Efficient and accurate computation of seismic traveltimes and amplitudes, *Geophys. Prosp.*, 52: 313-322.
- Chartrand, R. and Wohlberg, B., 2010. Total-variation regularization with bound constraints. *Acoustics Speech and Signal Processing (ICASSP), IEEE Internat. Conf.:* 766-769.
- Constable, S.C., Parker, R.L. and Constable, C.G., 1987- Occam's inversion: A practical algorithm for generating smooth models from electromagnetic sounding data. *Geophysics*, 52: 289-300.
- Figueiredo, M.A., Nowak, R.D. and Wright, S.J., 2007. Gradient projection for sparse reconstruction: Application to compressed sensing and other inverse problems. *IEEE J. Select. Top. Sign. Process.*, 1: 586-597.
- Gheymasi, H.M., Gholami, A., Siahkoohi, H.R. and Amini, N., 2016. Robust total-variation based geophysical inversion using split Bregman and proximity operators. *J. Appl. Geophys.*, 132: 242-254.
- Gholami, A. and Gazzola, S., 2022. Automatic balancing parameter selection for Tikhonov-TV regularization. *BIT Numer. Mathemat.*, 62: 1873-1898.
- Gholami, A. and Hosseini, S.M., 2013. A balanced combination of Tikhonov and total variation regularizations for the reconstruction of piecewise-smooth signals. *Sign. Process.*, 93: 1945-1960.
- Gholami, A. and Siahkoohi, H.R., 2010. Regularization of linear and non-linear geophysical ill-posed problems with joint sparsity constraints, *Geophys. J. Internat.*, 180: 871-882.
- Goldstein, T. and Osher, S., 2009. The split Bregman method for L1-regularized problems. *SIAM J. Imag. Sci.*, 2: 323-343.
- Gong, B., Schullcke, B., Krueger-Ziolek, S., Zhang, F., Mueller-Lisse, U. and Moeller, K., 2018. Higher order total variation regularization for EIT reconstruction. *Medic. Biol. Engineer. Comput.*, 56: 1367-1378.
- Hansen, P.C., 1998. *Rank-Deficient and Discrete Ill-Posed Problems: Numerical Aspects of Linear Inversion*. SIAM, Philadelphia.
- Hole, J.A. and Zelt, B.C., 1995. 3D finite difference reflection travel times. *Geophysics*, 121, 427-434.

- Kabanikhin, S.I., 2008. Definitions and examples of inverse and ill-posed problems. *J. Inv. Ill-Posed Problems*, 16: 317-357. DOI 10.1515 / JIIP.2008.069
- Liu, Y., Liu, C., Xie, C. and Zhao, Q.X., 2021. A hybrid regularization operator and its application in seismic inversion. *IEEE Access*, 9: 117378-117387.
- Maharramov, M. and Levin, S.A., 2015. Total-variation minimization with bound constraints. *arXiv preprint arXiv:1505.05694*.
- Morozov, V.A., 1984. *Methods for Solving Incorrectly Posed Problems*, Springer-Verlag, New York.
- Nocedal, J. and Wright, S. J., 2006, *Numerical Optimization*, 2nd ed. Springer Verlag, Heidelberg.
- Rawlinson, N. and Sambridge, M., 2003. Irregular interface parametrization in 3-D wide-angle seismic traveltimes tomography, *Geophys. J. Internat.*, 155: 79-92.
- Rockafellar, R.T., 1970. *Convex Analysis*. Princeton University Press, Princeton.
- Rudin, L.I., Osher, S. and Fatemi, E., 1992. Nonlinear total variation based noise removal algorithms. *Physica D: Nonlin. Phenom.*, 60: 259-268.
- Sambridge, M.S. and Kennett, B.L.N., 1990. Boundary value ray tracing in heterogeneous medium: A simple and versatile algorithm. *Geophys. J. Internat.*, 101: 157-168.
- Scales, J.A., Gersztenkorn, A. and Treitel, S., 1988, Fast Lp solution of large, sparse, linear systems: Application to seismic travel time tomography. *J. Computat. Phys.*, 75: 314-333.
- Sebudandi, Ch. and Toint, Ph.-L., 1993. Non-linear optimization for seismic traveltimes tomography. *Geophys. J. Internat.*, 115: 929-940.
- Sethian, J., 1996. A fast marching level set method for monotonically advancing front. *Proc. Nat. Acad. Sci.*, 93: 1591-1595.
- Sethian, J., 1999. Fast marching methods. *SIAM Review*, 41: 199-235,
- Sethian, J., 1999, *Level Set Methods and Fast Marching Methods: Evolving Interfaces in Computational Geometry, Computer Vision, and Materials Science*. Cambridge University Press, Cambridge.
- Sethian, J. and Popovici, A.M., 1999. 3-D traveltimes computation using the fast marching method. *Geophysics*, 64: 516-523.
- Stefan, W., Renaut, R.A. and Gelb, A., 2010. Improved total variation-type regularization using higher-order edge detectors. *SIAM J. Imag. Sci.*, 3: 232-251.
- Tibshirani, R.J. and Taylor, J., 2011. The solution path of the generalized lasso. *Ann. Statist.*, 39: 1335-1371.
- Tikhonov, A.N. and Arsenin, V.Y., 1977. *Solutions of Ill-Posed Problems*. Halsted Press, New York.
- Wahlberg, B., Boyd, S., Annergren, M. and Wang, Y., 2012. An ADMM algorithm for a class of total variation regularized estimation problems. *IFAC Proc. Vols.*, 45(16): 83-88.
- Vidale, J.E., 1988. Finite difference calculations of traveltimes, *Bull. Seismol. Soc. Am.*, 78: 2062-2076.
- Virieux, J. and Operto, S., 2009. An overview of full waveform inversion in exploration geophysics. *Geophysics*, 74(6): WCC1-WCC26.



**APPENDIX**

## Tikhonov- TV regularization with ADMM

The constrained problem for the Tikhonov- TV regularized objective function reads

$$\min_{\mathbf{x}} \|\mathbf{x}\|_2^2 + \lambda \|\mathbf{x}\|_1, \quad \text{Subject to } \mathbf{A}\mathbf{x} = \mathbf{b}, \quad (\text{A-1})$$

The ADMM iteration for solving the above-constrained problem is (See Aghamiry et al., 2019):

$$\mathbf{z}^k = \arg \min_{\mathbf{z}} \|\mathbf{z}\|_1 + \frac{\beta}{2} \|\mathbf{z} - \mathbf{A}^T \mathbf{u}^k + \mathbf{b}\|_2^2 \quad (\text{A-2})$$

$$\mathbf{z}^k \text{ solve via shrinkage operator} \quad (\text{A-3})$$

$$\mathbf{u}^k = \arg \min_{\mathbf{u}} \frac{\beta}{2} \|\mathbf{z}^k - \mathbf{A}^T \mathbf{u} + \mathbf{b}\|_2^2 \quad (\text{A-4})$$

$$\mathbf{z}^k = \mathbf{z}^k - \frac{1}{\beta} \mathbf{A}^T (\mathbf{u}^k - \mathbf{u}^{k-1}) \quad (\text{A-5})$$

$$\mathbf{u}^k = \mathbf{u}^k + \mathbf{A} (\mathbf{z}^k - \mathbf{z}^{k-1}) \quad (\text{A-6})$$